Prediction of Fiducial Parameter of PPG Signal—A Comparative Study Between Radial Basis and General Regression Neural Network Performance

Rashmi Rekha Sahoo and Palash Kumar Kundu

Abstract For assessing the human health, pulse wave monitoring has been used for years and years ago. Currently, the photoplethysmogram (PPG) is drawing attention because of its obvious advantages as non-invasive, simple structure, less volume, inexpensive, and convenient computer-based radial artery pulse diagnostic tool. PPG waveform contains significant information regarding cardiovascular systems about systolic, diastolic, and dicrotic index points, which helps to measure the physiological parameter like heart rate (beat), blood pressure, oxygen saturation (SpO2), and respiration in the blood. The PPG signal, which is an indicator of blood volume change, is captured with an IR light source and a photo detector, when arranged in reflective-type configuration. The fiducial parameters (time, amplitude of systolic, dicrotic and diastolic, and pulse wave time) are calculated by inflection points of the first and second-order derivatives of raw PPG waveforms. The present work focuses the applicability of artificial neural network as a predictor or estimator of these crucial fiducial parameters by using RBNN and GRNN, with modeling via Gaussian distribution function. Out of twenty subjects, training is done on ten subjects with RBNN and GRNN networks separately. The same has been tested with another ten subjects. The overall performance and accuracy of RBNN are found to be better than GRNN.

Keywords Photoplethysmogram · Fiducial parameters · Artificial neural network · GRNN · RBNN · Gaussian distribution function

1 Introduction

Because of tremendous development in nanotechnology advancement in miniature device, low energy consumption, high sensitivity, mobile, and tremendous computing power fostered an exponential increase growth of interest of wearable technology.

R. R. Sahoo (✉) · P. K. Kundu
Electrical Engineering Department, Jadavpur University, Kolkata, India

R. R. Sahoo
I&E Department, CET, Bhubaneswar, Odisha, India

S. Bhaumik et al. (eds.), *Proceedings of International Conference on Industrial Instrumentation and Control*, Lecture Notes in Electrical Engineering 815,
https://doi.org/10.1007/978-981-16-7011-4_10

Now, wearable bio-sensor-based[1] systems are the emerging trend, and its application covers from cardiovascular monitoring to military, battle, patient monitoring to many more. Photoplethysmography (PPG) is a non-invasive, vivo, and optical technique to detect disorders and diseases related to cardiovascular system to measure and monitor the physiological parameter such as blood pressure, oxygen saturation (SpO2), heart rate (beat), and respiration in the blood [2].

The proposal is to put the sensor, i.e., a IR transmitter (photodiode), which emits the light pulse periodically into the skin of fingertip, where some may be absorbed by tissue, some scattered, and some reflected (reflectance mode) to the photodetector (typically phototransistor). The absorption intensity utilizes Beer–Lambert's law [2], which illustrates when contraction of heart occurs blood comes out and enters into the blood vessel (artery) in accordance to the blood pressure. Hemoglobin (Hb) absorbs more light, so less light reflects and ultimately resistance of PD (photo resistor) increases. The PPG signal not only contains AC and DC components but also some noise components due to motion artifacts. AC component is caused by arterial blood in correspondence to every heartbeat. PPG waveform has three major fiducial components [3], namely systolic part, diastolic part, and dicrotic notch. These three parts are very much prominent in second derivative PPG (SDPPG) [4, 5].

There are some complex problem statements, where it is not so easy to establish an input and output relationship through mathematical modeling. For those situations, artificial neural network (ANN) plays a vital role. To have good prediction, precision in terms of RMS error and relative error [6] leads to statistical neural network (SNN). Depending upon the statistical method and probability theory, two major neural network, i.e., RBNN and GRNN are being used.

The present work thrusts the applicability of artificial neural network as an estimator of these crucial fiducial parameters of PPG by using *Radial Basis Neural Network* (RBNN) [6–8] and *General Regression Neural Network* (GRNN) [9, 10] with modeling done by a Gaussian function [11].

2 Methodology

The current work proposes the measurement of fiducial parameter like systolic (amplitude, time), diastolic (amplitude, time), dicrotic phases (amplitude, time), and pulse wave time (PWT) in photoplethysmography with experimental result [12]. The two maxima in PPG waveform show the systolic and diastolic peak, from which heart rate can be calculated. Dicrotic notch time and amplitude are calculated, when blood flows backward before the closer of aortic valve. Hence, each PPG cycle (waveform) having the fiducial parameter manifests the physiological performance of cardiovascular system of human body. The measurement process is illustrated in the subsequent paragraphs.

2.1 PPG Data Acquisition System

Module (HRM2511E Easy Pulse Plug in V1.1) is used as reflectance-type PPG sensor which is connected to analog channels of microcontroller ATMEGA328 board shown in Fig. 1a. The data acquisition program is implemented by ARDUINO embedded C language which runs on the ATMEGA328 embedded controller to capture PPG signal with sampling rate 250 Hz, as normal range of PPG signal is 0.5–4 Hz [13]. The microcontroller (ATMEGA328) transfers the data via USB and save (.txt) format containing the real-time signal sampled data of PPG waveform from subject.

Noise and Baseline Removal

After sampling at 250 Hz, PPG waveforms of four subjects are preprocessed by MATLAB 15b program through three steps. The steps are the following: (i) To remove high-frequency noise as a result of motion artifacts, filtered by a band pass type, having corner frequencies as 2 and 40 Hz, (ii) to have adequate level, automatic gain control (AGC) technique is used, and (iii) To remove wandering of baseline.

Beat Extraction

From the sampling data, local minima points are extracted with index number [13] and amplitude. One beat is formed between two consecutive index values. All the beats are stored in "ppg_beat_matrix.txt." Simply, saying ppg beat matrix will return all sample values over each respective cycle. Figure 3a shows the PPG of a particular person and its corresponding filtered signal. Beat 1–5 is correspondence to the information of each cycle.

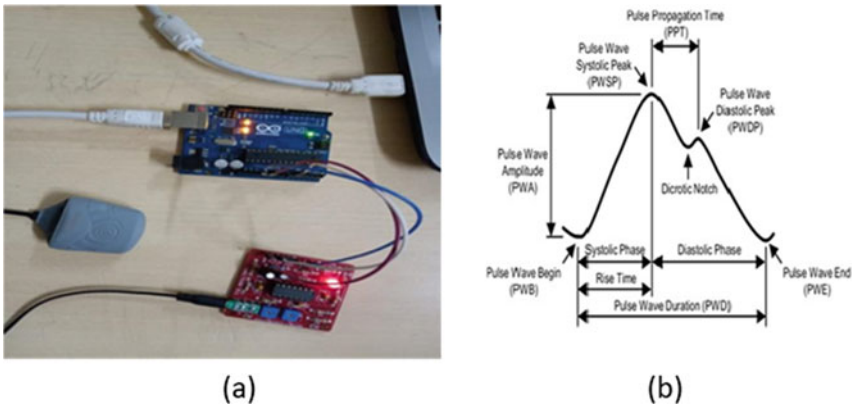

Fig. 1 **a** Data acquisition system for capturing PPG signal. **b** Fiducial parameter of PPG

3 Fiducial Parameter of PPG

A systolic peak amplitude, diastolic peak amplitude, dicrotic notch, systolic phase, diastolic phase, and pulse wave width are considered to major fiducial parameters for clinical analysis as shown in Fig. 2b.

3.1 Gaussian Modeling

Each PPG signal, after simulation-based signal processing, was modeled with a mixer set of two independent Gaussian functions as each cycle PPG has one systolic peak and one diastolic peak for better reconstruction and accuracy [13, 14]. The widely addressed probabilistic distribution function or Gaussian function or normal function at input x is characterized as:

$$f(x) = \frac{1}{\sigma_1\sqrt{2\Pi}} e^{\frac{-(x-\mu_1)^2}{2\sigma_1^2}} + \frac{1}{\sigma_2\sqrt{2\Pi}} e^{\frac{-(x-\mu_2)^2}{2\sigma_2^2}} \quad (1)$$

where mean $= \mu$, SD $= \sigma$, and variance $= \sigma^2$.

The philosophy behind this Gaussian distribution function is that it is highly used for initialization of random data and centered at around a value, i.e., the mean and usually set as zero. The modeling parameters (A, μ, and σ) were determined from sampled data as shown in Table 1a.

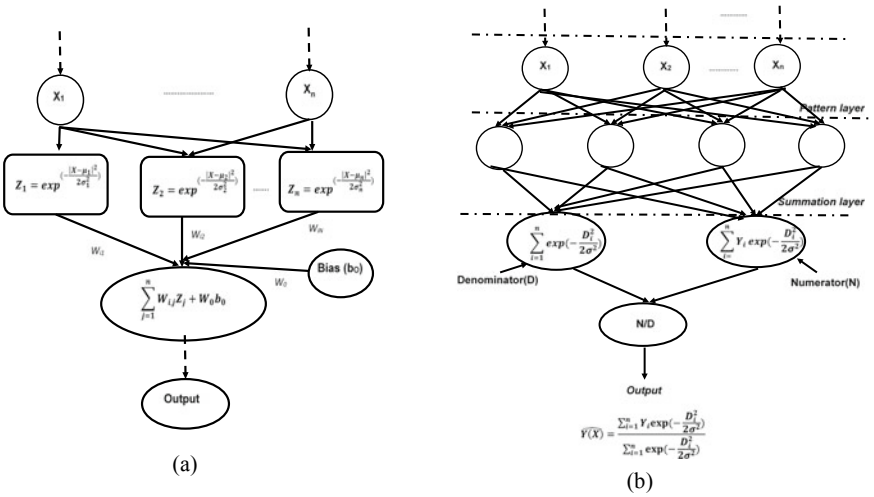

Fig. 2 **a** Radial basis neural network, **b** General regression neural network architecture

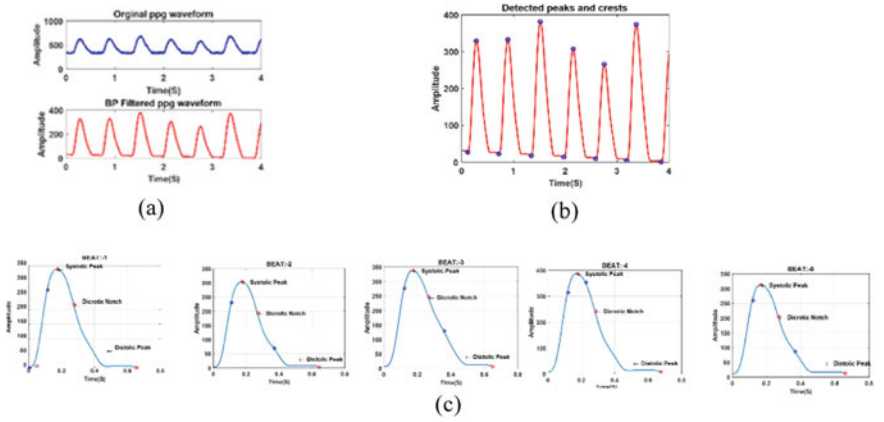

Fig. 3 **a** Noisy and filtered PPG signals, **b** detected peak and crests of PPG signal, **c** PPG waveforms of five beats for 50 years female subject.

Table 1a 2-Gauss model parameters and pulse wave time

Beat No.	2-Gauss model parameters						PTIME (s)
	A_1	μ_1	σ_1	A_2	μ_2	σ_2	
ID:50yr_high_bp_female_ppg(rest)							
1	0.6280	0.1490	0.0851	0.7010	0.1380	0.6980	0.4560
2	0.6630	0.3720	0.0849	0.6560	0.3230	0.9020	0.6640
3	0.4670	0.3880	0.0815	0.7840	0.6010	1.1000	0.7760
4	0.5280	0.2650	0.0805	0.7870	−0.1340	1.6500	0.5160
5	0.6430	0.4060	0.0864	0.6940	0.1820	0.9370	0.7160
ID:50yr_high_bp_male_ppg(rest)							
1	0.8820	0.1110	0.0680	0.9050	0.2250	0.2120	0.4560
2	0.9920	0.1170	0.0687	1.0100	0.3000	0.2110	0.4440
3	0.8000	0.1120	0.0656	0.8220	0.2110	0.3740	0.4480
4	0.8610	0.1140	0.0685	0.8740	0.2500	0.2760	0.4480
5	0.8140	0.1100	0.0630	0.8030	0.2460	0.3070	0.4520

Radial Basis Neural Network (RBNN)

Because of global approximation to input or output mapping, multilayer perceptron (MLP) network is not capable of fast learning. So, RBNN [11, 15] was proposed by Broomhead and Lowe in 1988 as shown in Fig. 2a. The network activity depends upon the activation function and weights. Generally, RBNN uses different activation functions [16] out of which radial basis function (RBF) is one.

Most widely used RBF using Gaussian function [16], having X as input pattern, "μ" as the center of function, and radius as σ^2, is shown in Fig. 2a with weight "w_j"

where output as $Y(x)$ (with bias b_0) and the Gaussian function ($z(x)$) are expressed as:

$$Y(x) = \sum_{j=1}^{n} w_j z_j(x) + w_0 b_0 \tag{2}$$

$$z(x) = \exp\left(\frac{-(x-\mu)^2}{2\sigma^2}\right) \tag{3}$$

Due to additive noise, when input data are corrupted RBNNs are preferably used for function approximation and pattern reorganization [17]. The architecture is shown in Fig. 2a. RBNNs are three-layered feedforward parallel network. Input layer is the first layer where individual neuron is fed with predictor variable. Next is a single hidden layer built with RBFs centered on a point. Location of input vector is calculated by Euclidean distance. The weight associated with the corresponding output from neuron of hidden layer is multiplied, and the sum gives the output of the NN is the last layer. In the RBNNs, first phase of the training is done in calculating RBF parameters (i.e., radius, coordinate of center), and in the second phase, the weights between hidden and output unit are estimated. The σ, μ, and the final weight are to be modeled.

General Regression Neural Network (GRNN)

GRNN which is coming under the category of probabilistic neural network (PNN) [15] is a feedforward supervised neural network. Because of feedforward architecture, the training becomes very fast. GRNN can be applied for interpolation, regression problem, prediction, and classification. GRNN can also be a good solution for online dynamical systems. GRNN is a regression estimator technique, where there is a Gaussian function to estimate the probability density function. Like BPNN, a GRNN [10] do not do repetitive training. The topology of GRNN has four layers. It is clearly visible in Fig. 2b that it has input layer, pattern layer, summation layer, and output layer. The measured X is fed to the first input layer neuron. Then, second layer (1st hidden layer) having N nodes for N sampled data, known as a pattern layer, is connected to first layer. The squaring of difference result (D) is taken between input vector, Xi, and the vector assigned to the node, and Xj for jth sample in training data is fed to exponential function with a smoothing factor (σ). This output patterns are given to the two sum units of summation layer (second hidden layer). First, summation neuron gives the sum of product of the second layer outputs and observed output y_i. Likewise, second summation neuron is the sum of the second layer activation. Output layer is the last one to divide the result of two sum node to predict the result, i.e., to estimate $Y(X)$ as:

The output is given by:

$$\widehat{Y(X)} = \frac{\sum_{i=1}^{n} Y_i \exp\left(-\frac{D_i^2}{2\sigma^2}\right)}{\sum_{i=1}^{n} \exp\left(-\frac{D_i^2}{2\sigma^2}\right)} \tag{4}$$

4 Result and Analysis

PPG waveforms are recorded from fingertips of ten subjects (five male and five female) with age group ranging from 22 to 57 years. The stored datasets are filtered with second-order band pass filter having corner frequency from 2 to 40 Hz. The filtered datasets are corrected with gain adjustment multiplying factor to main peak-to-peak value to its original PPG waveform as shown in Fig. 3a. The local minima of filtered dataset in PPG waveform are detected as shown in Fig. 3b. The sampled datasets within successive minima point are extracted and stored in an array PPG beat matrix. The first and second derivatives of sampled datasets within each beat are computed.

The filtered PPG waveform data samples for ten subjects are converted to beat matrix array, the column of which is used as one period of PPG waveform, called pulse time and stores the total data samples in it. Thus, dataset for five beats (i.e., five PPG waveform cycles) is stored into ppg beat matrix file. Each PPG beat is modeled with mixtures of two Gaussian functions as given by Eq. 1, which results six coefficients. The model coefficients are considered the features of PPG waveform. Thus, all beats are modeled by Gaussian method, and they are stored into data file, where each record in file consists of six model coefficients, and the PPG pulse time period in second.

The fiducial point of interest is computed with the help of index located at +ve and −ve zero crossing points first-order derivative and −ve peak of second-order derivative of PPG waveform for all the beats as shown in Fig. 3c. The fiducial points of five subjects as systolic peak and time, dichotic notch peak and time, and diastolic peak and time are shown in Table 1b. Systolic and diastolic phase durations, and pulse wave time.

The Gaussian model as features of input and fiducial parameters (time and amplitude) as target outputs is utilized for training radial basis and generalized regression neural networks. The trained RBNN and GRNN networks are tested by applying beat-wise feature input of 50 years female subject. The predicted values of fiducial parameters by RBNN and GRNN are shown in Tables 2a and 2b, respectively. The errors with respect to original value as computed for all the beats are shown in Tables 3a and 3b. It is clearly observed that performance by RBNN is better as the errors found in case RBNN are much less than that by GRNN.

Table 1b Time and amplitude of fiducial parameters and pulse wave time

Beat No.	Fiducial parameters						PTIME (s)
	Systolic		Dicrotic		Diastolic		
	Time (s)	Peak	Time (s)	Level	Time (s)	Level	
ID:50yr_high_bp_female_ppg(rest)							
1	0.152	1.320	0.224	1.020	0.456	0.573	0.456
2	0.372	1.310	0.444	1.000	0.664	0.573	0.664
3	0.388	1.210	0.464	1.000	0.776	0.584	0.776
4	0.264	1.260	0.336	0.996	0.516	0.671	0.516
5	0.404	1.290	0.480	0.975	0.716	0.518	0.716
ID:50yr_high_bp_male_ppg(rest)							
1	0.124	1.560	0.180	1.240	0.456	0.235	0.456
2	0.128	1.460	0.176	1.230	0.444	0.231	0.444
3	0.120	1.550	0.180	1.150	0.448	0.517	0.448
4	0.124	1.540	0.176	1.240	0.448	0.516	0.448
5	0.116	1.460	0.172	1.120	0.452	0.493	0.452

Table 2a Time and amplitude of fiducial parameters and pulse wave time predicted by RBNN

Beat No.	Fiducial parameters predicted by RBNN						PTIME (s)
	Systolic		Dicrotic		Diastolic		
	Time (s)	Peak	Time (s)	Level	Time (s)	Level	
ID:50yr_high_bp_female_ppg(rest)							
1	0.152	1.320	0.224	1.020	0.456	0.573	0.456
2	0.372	1.310	0.444	1.000	0.664	0.573	0.664
3	0.388	1.210	0.464	1.000	0.776	0.584	0.776
4	0.264	1.260	0.336	0.996	0.516	0.671	0.516
5	0.404	1.290	0.480	0.975	0.716	0.518	0.716
ID:50yr_high_bp_male_ppg(rest)							
1	0.124	1.560	0.180	1.240	0.456	0.235	0.456
2	0.128	1.460	0.176	1.230	0.444	0.231	0.444
3	0.120	1.550	0.180	1.150	0.448	0.517	0.448
4	0.124	1.540	0.176	1.240	0.448	0.516	0.448
5	0.116	1.460	0.172	1.120	0.452	0.493	0.452

5 Discussion

In present work, captured PPG signal from index finger and later waveform data has been cleaned from baseline and noise. When the heart muscle contracts, blood flows in peripheral tissues and changes the fiducial parameter of PPG (i.e., systolic, diastolic

Table 2b Time and amplitude of fiducial parameters and pulse wave time predicted by GRNN

Beat No.	Fiducial parameters predicted by GRNN						PTIME (s)
	Systolic		Dicrotic		Diastolic		
	Time (s)	Peak	Time (s)	Level	Time (s)	Level	
ID:50yr_high_bp_female_ppg(rest)							
1	0.203	1.420	0.269	1.100	0.521	0.493	0.521
2	0.317	1.320	0.389	1.020	0.634	0.539	0.634
3	0.370	1.260	0.445	1.000	0.717	0.567	0.717
4	0.274	1.260	0.346	0.996	0.533	0.658	0.533
5	0.325	1.320	0.398	1.020	0.640	0.542	0.640
ID:50yr_high_bp_male_ppg(rest)							
1	0.145	1.630	0.207	1.270	0.484	0.275	0.484
2	0.150	1.690	0.216	1.310	0.498	0.218	0.498
3	0.146	1.570	0.207	1.220	0.478	0.350	0.478
4	0.144	1.610	0.206	1.260	0.481	0.300	0.481
5	0.144	1.580	0.205	1.240	0.477	0.334	0.477

and dicrotic index, and pulse transit time) over every cycle or beat. Depending upon sex, age and movement condition or rest pulse transit time and HRV parameters varies. Hence, for diagnosis of cardiovascular diseases, PPG waveform dataset can be used to monitor HRV. Fiducial parameters (time and amplitudes of index points) of PPG signal were computed from first-and second-order derivative of PPG signal [5], which requires the large computation time for processing PPG waveform dataset extraction of sampled dataset into beat matrix format and thereafter locating the index points at systolic, diastolic, and dichroitic regions. The ANN method can reduce the computation time for determining the fiducial parameters. However, instead of using raw data relating sampled data of PPG waveform, features have been extracted after modeling it by the sum of two Gaussian functions, which yields the six coefficients (e.g., A_1, μ_1, σ_1 and A_2, μ_2, σ_2) and pulse transit time (PTIME). The features as input vectors with their corresponding fiducial parameter values of systolic, diastolic, dichroitic regions (e.g., time and amplitudes), and pulse transit time (PTIME) as target vectors are utilized to train general regression and radial basis neural networks separately. The radial basis (RBNN) and general regression (GRNN) network are a good alternative and advantageous to the multilayer perception back Propagation (MLP BP) network as these has only three-layer architecture, and it has a much faster training process compared to the MLP. The trained networks are tested by feature of one subject randomly for prediction about their fiducial parameter. The percentage error with respect to original values as determined analytically has been found. It is observed that the performance of RBNN is better as the error is very low compared to that by GRNN. The RBNN and GRNN methods can also be used for prediction of HRV parameters (e.g. PPG augmented index for arterial stiffness measurement, mean value of P-P interval time, standard deviation of successive P-P interval time,

Table 3a Error in fiducial parameters by RBNN

Beat No.	Error (%) in fiducial parameters by RBNN						PTIME (s)
	Systolic		Dicrotic		Diastolic		
	Time (s)	Peak	Time (s)	Level	Time (s)	Level	
ID:50yr_high_bp_female_ppg(rest)							
1	5.79E−12	1.13E−12	−1.85E−11	3.91E−11	−9.50E−13	1.46E−10	−1.31E−12
2	3.86E−12	2.74E−12	1.81E−11	−1.29E−11	1.99E−12	−7.25E−12	1.49E−12
3	9.59E−13	−1.69E−12	9.01E−12	−7.34E−12	3.15E−13	1.71E−11	6.87E−13
4	1.87E−12	−2.06E−12	1.19E−11	1.32E−11	2.58E−13	2.78E−11	5.59E−13
5	1.80E−12	1.95E−12	3.89E−12	1.52E−11	1.55E−13	9.72E−11	1.86E−13
ID:50yr_high_bp_male_ppg(rest)							
1	3.18E−12	4.49E−12	−2.87E−11	1.66E−11	−2.90E−12	5.55E−10	−1.70E−12
2	2.04E−12	3.25E−12	9.75E−12	2.85E−11	−7.50E−14	2.01E−10	−8.50E−13
3	4.39E−12	2.53E−12	6.82E−12	1.86E−11	−3.15E−12	7.78E−11	−2.33E−12
4	1.75E−12	3.90E−12	−6.40E−12	2.27E−11	−7.68E−13	1.59E−10	−3.47E−13
5	4.18E−12	5.75E−12	−3.71E−12	7.27E−12	−1.06E−12	1.03E−10	−1.82E−12

Table 3b Error in fiducial parameters by GRNN

Beat No.	Error (%) in fiducial parameters by GRNN						PTIME (s)
	Systolic		Dicrotic		Diastolic		
	Time (s)	Peak	Time (s)	Level	Time (s)	Level	
ID:50yr_high_bp_female_ppg(rest)							
1	33.6000	7.2900	20.0000	7.8600	14.2000	14.1000	−14.2000
2	14.8000	1.2800	12.5000	2.0800	4.4900	5.8700	4.4900
3	4.5500	3.8900	4.1300	−0.0472	7.6600	2.8400	7.6600
4	3.7400	−0.1770	3.0100	0.0463	3.2100	1.8200	−3.2100
5	19.5000	2.1800	17.2000	4.1800	10.6000	4.6900	10.6000
ID:50yr_high_bp_male_ppg(rest)							
1	−16.5000	4.6100	15.0000	3.1000	6.2200	17.1000	−0.0284
2	17.1000	15.6000	22.5000	6.4400	12.2000	5.4700	−0.0542
3	21.5000	1.3100	14.9000	6.0300	6.6700	32.3000	−0.0299
4	16.2000	4.8200	17.0000	1.3600	7.4000	41.9000	−0.0331
5	23.8000	8.0400	19.0000	10.0000	5.5700	32.3000	−0.0252

parentage of successive P-P interval time, which differs from more than that by 50 ms, standard deviation of instantaneous and long term P-P interval variability).

References

1. Rawal, V., Dhamija, A., Gupta, S.: Recent advances in wearable bio-sensors application. Int. J. Sci. Res. Comput. Sci. Eng. Inf. Technol. **1**(5), 154–159 (2012). ISSN: 2278-0882
2. Yang, Y., Zhu, J., Zhu, P.: SpO2 and heart rate measurement with wearable watch based on PPG. In: IEEE Conference 2015 IET International Conference on Biomedical Image and Signal Processing (2015)
3. Chan, G., Middleton, P., Celler, G.: Automatic detection of left ventricular ejection time from a finger photoplethysmographic pulse oximetry waveform, comparison with Doppler aortic measurement. Physiol. Meas. **28**, 1–14 (2007)
4. Toshiaki, O., Tomoyuki, K., Masao, K., Chikao, I.: Utility of second derivative of the finger photoplethysmogram for the estimation of the risk of coronary heart disease in the general population. Circ. J. **70**, 304–310 (2006)
5. Hashimoto, J., Chonan, K., Aoki, Y.: Pulse wave velocity and the second derivative of the finger photoplethysmogram in treated hypertensive patients: their relationship and associating factors. J. Hypertens. **20**(12), 2415–2422 (2002)
6. Celikoglu, H.B.: Application of radial basis function and generalized regression neural networks in non-linear utility function specification for travel mode choice modelling. Math. Comput. Model. **44**, 640–658 (2006)
7. Sun, N., Zhang, S., Peng, T., Zhou, J., Sun, X.: A composite uncertainty forecasting model for unstable time series: application of windspeed and streamflow forecasting. IEEE Open Access J. **8**, 209253–209266 (2020)

8. Ge, Y., Yang, L., Ma, X.: A novel terminal sliding mode control based on RBF neural network for the permanent magnet synchronous motor. In: 2018 International Symposium on Power Electronics Electrical Drives Automation and Motion (SPEEDAM), pp. 1227–1232 (2018)
9. Hannan, S., Manza, R., Ramteke, R.: Generalized regression neural network and radial basis function for heart disease diagnosis. Int. J. Comput. Appl. **7**(13) (2010)
10. Liu, F., Si, Y., Luo, T.: The ECG identification based on GRNN. In: IEEE International Conference on Communication Systems (ICCS) (2019). ISBN: 978-1-5386-7865-7
11. Korürek, M., Dogan, B. : ECG beat classification using particle swarm optimization and radial basis function neural network. Expert Syst. Appl. **37**, 7563–7569 (2010)
12. Qawqzeh, Y., Uldis, R., Alharbi, M.: Photoplethysmogram second derivative review: analysis and applications. Acad. J. Sci. Res. Essays **10**(21), 633–639 (2015)
13. Bhowmick, S., Kundu, P., Mandal, D.: IoT assisted real time PPG monitoring system for health care application. In: 2021 IEEE Second International Conference on Conference on Control Measurement and Instrumentation (CMI), pp. 122–127 (2021)
14. Kundu, P., Gupta, R.: Electrocardiogram synthesis using Gaussian and Fourier models. In: International Conference on Research in Computational Intelligence and Communication Networks (ICRCICN), pp. 312–317. IEEE Computer Society (2015)
15. Blanco, M., Miranda, V., Vargas, G.: Generalized regression neural networks with application in neutron spectrometry. In: Artificial Neural Networks—Models and Applications. InTech-Open Science|Open Mind, Chap. 3, pp. 49–83 (2016)
16. Spetch, D.F., Romsdhal, H.: Experience with adaptive probabilistic neural networks and adaptive general regression neural networks. IEEE Int. Conf. Neural Netw. **2**, 1203–1208 (1994)
17. Spetch, D.F., Shapiro, P.: Generalization accuracy of probabilistic neural networks compared with back propagation networks. In: IJCNN-91-Seattle International Joint Conference on Neural Networks, vol. 1, pp. 887–892 (1991)